Hydrogen Peroxide/Zero Valent Iron/Persulfate Approach for Dye Degradation: Key Operating Parameter and Synergistic Effect

Mehdi Ahmadi

Ahvaz Jundishapur University of Medical Sciences: Ahvaz Jondishapour University of Medical Sciences

rozhan feizi (rozhanfeizi@gmail.comb)

Ahvaz Jundishapur University of Medical Sciences: Behbahan University of Medical Sciences

https://orcid.org/0000-0002-9281-0451

Research Article

Keywords: Azo dyes, zero- valent iron (ZVI), persulfate, hydrogen peroxide, wastewaters

Posted Date: May 24th, 2021

DOI: https://doi.org/10.21203/rs.3.rs-468460/v1

Abstract

Azo dyes due to the presence of benzene ring, toxicity, mutagenicity, carcinogenicity and low biodegradability have become a major problem in the aqueous environment. In this study, Zero Valent Iron (ZVI) was employed as a catalyst to activate persulfate (PS) and hydrogen peroxide (H_2O_2) for removal of Sunset Yellow (SY) from aqueous solutions using integrated H_2O_2/ZVI/PS process. The effects of operational parameters (solution pH, H_2O_2 concentration, PS concentration, and ZVI dose) were studied on SY removal. According to the results, about 100% efficiency was obtained by the H_2O_2/ZVI/PS for dye removal at: pH = 3, ZVI 50 mg/L, 1 mM H_2O_2 concentration, 1 mM PS concentration, and 30 min reaction time. The kinetic study implied that the H_2O_2/ZVI/PS process followed the first-order kinetic model. The total organic carbon (TOC) test showed that about 65% of mineralization was achieved after 30 min. Moreover, the ZVI particles showed a suitable efficiency after five cycles, and hence, it can be used as an eco-friendly, cost effective and reusable catalyst for the treatment of wastewaters contaminated with such dyes.

1 Introduction

Azo dyes are about 70% of the synthetic dyes used in the textile industries and known as environmentally persistent compound (Maroudas et al. 2020). These compounds have an azo group (–N = N–) and aromatic rings in their structure, which can cause environmental problems (Matyszczak et al. 2020). Hence, various methods have been used for wastewater treatment containing colored compounds. Advanced oxidation processes such as ozonation, UV/O_3, UV/H_2O_2, Fe^{2+}/H_2O_2, and UV/O_3/ H_2O_2 has received remarkable attention for the removal of azo dyes (Chang et al. 2006). Over the last few decades, chemical oxidants such as ozone, hydrogen peroxide (HP) and persulfate (PS) through the production of hydroxyl radicals ($OH^{\bullet}$) and sulfate radicals ($SO_4^{\bullet -}$) has been applied for removing dyes from large volumes of wastewater (Khan et al. 2013; Wordofa et al. 2017; Tariq & Khan 2020). Hydrogen peroxide (H_2O_2) with oxidation potential 2.07 V is a common oxidizing agent used in the oxidation of organic compounds (Hou et al. 2012). In recent years, persulfate as a strong oxidizing agent with a redox potential of 2.01 V has been introduced for degradation of persistent pollutants. Moreover, persulfate due to its characteristics such as cheapness, non-selective oxidation, and high stability of the produced radical under various conditions and high solubility compared to other oxidants makes it an attractive option for the oxidation of organic contaminants (Oh et al. 2009). Organic matter degradation by PS is achieved at slow kinetics at room temperature. Therefore, it is necessary to activate PS for accelerating the process. The PS can be activated by heat (Eq. 1), UV light (Eq. 2) and transition metals (Me^{2+}) according to Eq. 3. The activated PS produces sulfate radical (SO_4^{-}) with highly reactive oxygen species (E0 = 2/07 V), which can convert the contaminant compounds into harmless products (Oh et al. 2011).

$S_2O_8^{2-} \rightarrow 2SO_4^{\bullet -}$ (30°C < T < 99°C) (1)

$S_2O_8^{2-} \rightarrow 2SO_4^{\bullet -}$ (hv ≈ 254 nm) (2)

$S_2O_8^{2-} + Me^{n+} \rightarrow SO_4^{\bullet -} + Me^{(n+1)} + SO_4^{2-}$ (3)

Among metals, the iron is a most usage related which requires high value, high volume production of sludge and consumption of $SO_4^{\bullet}$ radicals at high concentrations of the main problems is this activator (Oh et al. 2010). Due to the small particle size, high density, high specific surface area and high efficiency of zero-valent iron particles (ZVI), it can act as a constant source of Fe^{2+} and react with iron continuously for removing a wide range of contaminants (according to the Eqs. 4 and 5) (Zha et al. 2014; Raji et al. 2020).

$S_2O_8^{2-} + Fe^0 \rightarrow Fe^{2+} + 2SO_4^{2-}$ (4)

$S_2O_8^{2-} + Fe^{2+} \rightarrow SO_4^{\bullet -} + Fe_3^{+} + SO_4^{2-}$ (5)

Therefore, due to the specific features of the advanced oxidation process at the removal of organic compounds, especially the color compounds and due to the lack of sufficient information to compare different oxidants such as H_2O_2 and PS activated by zero-valent iron, thus the aim of this study was Hydrogen peroxide/zero valent iron/persulfate approach for dye degradation: key operating parameter and synergistic effect.

2 Materials And Methods

2.1 Reagents

Sunset yellow (SY, $C_{16}H_{10}N_2Na_2O_7S$) (Fig. 1) was obtained from Alvan Sabet Company (Iran). Ps (98%) was purchased from Panreac (Spain). Iron metal powder (with a purity of 97%) was purchased from Sigma–Aldrich, Hydrogen peroxide (35%), sulfuric acid (98%), ethanol (EtOH) and tert-butyl alcohol (TBA) were obtained from Merck C. Sodium bicarbonate ($NaHCO_3$), sodium chloride (NaCl), sodium nitrate ($NaNO_3$), sodium nitrite ($NaNO_2$), sodium sulfate (Na_2SO_4), sodium bicarbonate ($NaHCO_3$) were prepared from Samchun Inc.

2.2. Experimental Procedures

In the present study, all experiments were conducted in a batch reactor at atmospheric temperature and pressure containing 50 mL of sunset yellow dye, which includes different concentration of zero valent iron particles (25 to 150 mg/L), hydrogen peroxide (0.25 to 2 mM) and persulfate (0.25 to 2 mM). Initial pH of dye solution was adjusted using 1 N sodium hydroxide and sulfuric acid solutions using a digital pH meter (EUTECH-pH 1500). Afterward, in order to investigate the effects of operating parameters on the H_2O_2/ZVI/PS process, some experiments were performed to determine the optimal conditions for SY removal. The zero valent iron particles was collected from the solution using a magnet.

2.3 Analytical Method

In order to determine the concentration of residual dye in the aqueous phase, liquid samples were withdrawn periodically (in six 5- min intervals) and then read by using an UV – vis, UV/Vis spectrophotometer (DR-5000, HACH, USA). The characteristic wavelength for this compound is 482 nm. Then the removal efficiency of dye (%) was obtained in accordance with Eq. (6):

Residual dye (%) = $(C_0-C_t)/C_0$ *100 (6)

Where, C_0 is the initial dye concentration, and C_t is the dye concentration at times. TOC was measured using a Shimadzu VCHS/CSN Japan analyzer by oxidative combustion at 680°C using an infrared detector (Feizi et al. 2019).

3 Results And Discussion

3.1 Effect of pH on decolorization

In chemical processes, the solution pH is an important element affecting the removal of organic compounds efficiency. The effect of solution pH on the degradation rate of SY was investigated on the process performance (SY concentration: 50 mg/L, H_2O_2: 1 mM, PS 1 mM and ZVI: 50 mg/L). The results are illustrated in Fig. 2. As can be seen here, the highest removal efficacy (99.71%) was achieved at pH = 3 in the H_2O_2/ZVI/PS process. So that the dye removal efficiency decreased significantly with increasing pH. Previous studies have indicated that the solution pH has a considerable effect on the stability of H_2O_2, OH• concentration and the iron species in the solution (Malakootian *et al.* 2020). Generally, the acidic condition causes the fast disappearance of Fe^0 and the release of more Fe^{2+} in accordance with Eq. (7), resulting in the production of more free radicals ($SO_4^{\bullet-}$ and $OH^{\bullet}$) for the better dye removal performance that can be generated according to Eqs. (5,8) (Ike et al. 2018). In contrast, under alkaline conditions, Fe^{2+} and Fe^{3+} are almost insoluble that causes the iron ions rapidly in solid and colloidal ($FeOH^+$) form and affects their ability to activate PS Eq. (9) (Li et al. 2013), thereby significantly slow down the dye degradation. In addition, $S_2O_8^{2-}$ decomposition at acidic pH occurred through acid-catalyzed reactions (Eqs. (10 and 11)). On the other hand, $^{\bullet}OH$ can be generated through $SO_4^{\bullet-}$ reaction with H_2O (Eq. 12) or HO^- (Eq. 13) at alkaline pH, resulting in less $SO_4^{\bullet-}$ available for decolorization (Anipsitakis & Dionysiou 2004).

$Fe^0 + H^+ \rightarrow Fe^{2+} + H_2$ (7)

$Fe^{2+} + H_2O_2 \rightarrow Fe^{3+} + OH^- + OH\bullet$ (8)

$Fe^{2+} + H_2O \rightarrow FeOH^+ + H^+$ (9)

$S_2O_8^{2-} + H^+ \rightarrow HS_2O_8^-$ (10)

$2H_2O_2 \rightarrow 2H_2O + O_2$ (11)

$SO_4^{\bullet -} + H_2O \rightarrow SO_4^{2-} + OH\bullet + H^+$ (12)

$SO_4^{\bullet -} + HO^- \rightarrow SO_4^{2-} + OH\bullet$ (13)

3.2 Effect of oxidants concentration

In Advanced oxidation processes (AOPs), the concentration of oxidants directly affects the amounts of generating free radicals. In addition, choosing optimal dosage of oxidants can obviously decrease the process costs (Li et al. 2017). The effect of the H_2O_2 and PS concentration in the range of 0.25–2 mM were investigated on the H_2O_2/ZVI/PS process efficiency for decolorization. As shown in Fig. 3a, the increasing H_2O_2 dosage enhances the process efficiency for decolorization, due to the fact that H_2O_2 is the source of hydroxyl radicals. So that the obvious increase of H_2O_2 dosage increases the concentration of reactive hydroxyl radicals (•OH), and then decolorization. Nonetheless, the dye removal rate decreased with further increase in the H_2O_2 concentration from 1mM to 1.5 mM, and even with the further increase in H_2O_2 concentration up to 2 mM. The reduced oxidation efficiency at higher H_2O_2 values can be attributed to the: (i) the reaction of excess ferrous iron with excess H_2O_2, (ii) scavenging effect of •OH by H_2O_2, therefore, one or more of side reactions occur under such conditions (Eqs. (14)–(18)), which results in the formation of oxidants like HOO and O^{2-}, which has much lower oxidation potential compared with active hydroxyl radicals (•OH) (de Souza Santos et al. 2015). In H_2O_2/ZVI/PS process, more persulfate concentration leads to more contact between ZVI and PS. Therefore, more sulfate radicals were generated in aqueous solution. Nonetheless, as shown in Fig. 3b, as the PS dosage increased, the dye removal decreased, and even with the further increase in PS concentration, the efficiency of decolorization decreased, which could be attributed to the: (i) reaction between $S_2O_8^{2-}$ and $SO_4^{-\bullet}$ (Eq. (19)), (ii) the recombination between two $SO_4^{-\bullet}$ (Eq. 20) (Wu et al. 2019). Thus, it can be concluded though entering a high amount of PS into the system is theoretically associated with a high decolorization rate. But the gain effect is limited and the quantity of PS added is just useful up to a defined concentration, after which it has negative effects. Therefore, PS concentration of 1 mM is selected as the optimum concentration for the decolorization.

$Fe^0 + H_2O_2 \rightarrow Fe^{2+} + 2O^-$ (14)

$Fe^{2+} + H_2O_2 \rightarrow Fe^{3+} + \bullet OH$ (15)

$H_2O_2 + \bullet OH \rightarrow HO_2/\ O_2^{-\bullet} + H_2O$ (16)

$Fe^{3+} + HO_2 \rightarrow Fe^{2+} + O_2 + H^+$ (17)

$Fe^{2+} + HO_2 \rightarrow Fe^{3+} + HO_2^-$ (18)

$SO_4^{-\bullet} + S_2O_8^{2-} \rightarrow SO_4^{2-} + S_2O_8^- + H^+$ (19)

$SO_4^{-\bullet} + SO_4^{-\bullet} \rightarrow S_2O_8^{2-}$ (20)

3.3 Effect of ZVI dose

In order to evaluate the effect of ZVI dose on the H_2O_2/ZVI/PS process for the dye removal, experiments were carried out at various catalyst concentrations in the range between 25 mg/L and 150 m/L, under constant conditions (SY concentration: 50 mg/L, solution pH: 3, H_2O_2 dosage: 1 mM, PS: 1 mM and ZVI: 50 mg/L. As shown in Fig. 4, the increasing concentration of ZVI enhanced the process efficiency for decolorization. Nonetheless, the further increase in ZVI concentration diminished the process performance. This result is due to the fact that with increasing ZVI dose the number of surface active sites also increased. This phenomenon enhanced H_2O_2 and PS decomposition and the production of hydroxyl and sulfate radicals in accordance with Eqs. (14, 15, and 21), which consequently improved the decolorization efficiency. However, excessive dosage of ZVI causes particle aggregation and the scavenging of •OH and $SO_4^{\bullet -}$ radicals through the undesirable reaction leads to a decrease in dye removal efficiency (Eqs. 23, and 22) (Babuponnusami & Muthukumar 2012; Zha et al. 2014).

$Fe^0 + S_2O_8^{2-} \rightarrow Fe^{2+} + 2SO_4^{2-}$ (21)

$Fe^{2+} + {\bullet}OH \rightarrow Fe^{3+} + OH^-$ (22)

$Fe^0 + SO_4^{-\bullet} \rightarrow Fe^{3+} + SO_4^{2-}$ (23)

3.4 The kinetic model and synergistic effect

The performance of decolorization by different processes include ZVI, PS, H_2O_2, ZVI/ H_2O_2, ZVI /PS, H_2O_2/ PS, and H_2O_2/ZVI/PS was evaluated under identical experimental conditions (solution pH 3, initial SY concentration 50 mg/L, ZVI 50 mg/L, H_2O_2 1 mM, PS 1 mM, and reaction time 30 min) (Fig. 5 (a)). It can be seen that the treatment of H_2O_2 or PS alone had a negligible effect on the decolorization process, which may due to related to the absence of generation of oxidizing radicals (i.e., OH and SO_4). Furthermore, With Fe0 composite only, about 15% removal was observed mainly due to surface adsorption. The results further proved synergistic effect existed in the binary PS/H_2O_2, Fe0/PS, and Fe0/H_2O_2 systems, In the presence of both PS and H_2O_2, the decolorization reached 45% after 30 min reaction. The low efficiency of PS/H_2O_2 system may be explained by the short treatment time, which with

adding catalyst could be enhanced significantly (Wang & Xu 2012). In PS/Fe0 system plenty of H + ion released from hydrolysis of persulfate and resulting in the decrease of dissolved pH (Eqs. (24) and (25)), which could the accelerate Fe0 corrosion continuously. And then the released iron corrosion products could activate persulfate to produce $SO_4^{\bullet -}$ (Zhao et al. 2010). On other hand released iron corrosion products can in Fe^0/H_2O_2 systems, catalyze the Fenton reaction in the presence of H_2O_2 for the generation of oxidizing radicals (i.e., •OH and $SO_4^{\bullet -}$). Also, H_2O_2 can continuously the corrosion rate of Fe0 accelerate and prepare the fresh Fe0 from passivation (Desai et al. 2016; Guo et al. 2016). Since, the Fenton or Fenton-like reaction usually under the acidic condition is performed, therefore in the presence of PS can be found the strong synergistic effect between Fe0 and H_2O_2 through hydrolysis of persulfate and release H + ion under the acidic condition (Matzek & Carter 2016). According to the results, the highest removal efficiency (100%) was obtained by Fe0 /PS/H_2O_2 process after 30 min reaction by synergistic effects between persulfate and H_2O_2, and adding catalyst, which can be attributed to the activation of H_2O_2 with Fe^{2+}/Fe^{3+} in the presence of Fe species (Eqs. (16, 17, 26, and 27)) and reaction between HO_2^- with PS that results in the production of superoxide radicals (Eq. (28)) (Wang & Xu 2012; Tang et al. 2016). In this regard, similar results also found by LI, Jun et al. for the degradation of PNP (p-nitrophenol). In the mentioned study, 99.9% after 6 min treatment obtained that there is a strong synergistic effect in the Fe^0/H_2O_2/persulfate process (Li et al. 2017). On the other hand, In order to determine the speed of chemical reaction, the kinetic of first-order for decolorization was calculated using Eq ($\ln C_0/C_t = kt$). (39–41). Where C_0 and C_t represent the initial and residual dye concentration (mg/L), t is the reaction time (min), and K the corresponding rate constant (h^{-1}). According to Table 1, the first-order kinetic model was for all processes with constant rate (R^2) of more than 0.9. Figure 5 (b) displays the linear forms of first-order model that according to the results, the rate constants (0.1919 min^{-1}) of H_2O_2/ZVI/PS process much more than that of other systems.

$$H_2O + S_2O_8^{2-} \rightarrow 2HSO_4^- + 1/2O_2 \quad (24)$$

$$HSO_4^- \rightarrow SO_4^{2-} + H^+ \quad (25)$$

$$HO_2\cdot \rightarrow O_2\cdot^- + H^+ \quad (26)$$

$$Fe^{3+} + H_2O_2 \rightarrow Fe^{2+} + HO_2\cdot + H^+ \quad (27)$$

$$HO_2^- + S_2O_8^{2-} \rightarrow SO_4^{2-} + SO_4^{\cdot -} + H^+ + O_2^{\cdot -} \quad (28)$$

Table 1 The rate constant, *R*-squared of kinetic models.

First-order (*Ln $C_0/C_t = k_1t$*)		
	R^2	$k_{obs}(min^{-1})$
ZVI	*0.971*	*0.0073*
PS	*0.976*	*0.0100*
H_2O_2	*0.972*	*0.0115*
H_2O_2/ PS	*0.990*	*0.0194*
ZVI/PS	*0.952*	*0.0459*
ZVI/ H_2O_2	*0.978*	*0.0661*
PS/ZVI/ H_2O_2	*0.902*	*0.1991*

3.5 Effect of anions

Anions in aquatic environments are commonly considered to be radical scavengers, which could play a detrimental role in the performance of AOPs (Cui et al. 2016). Thus, in the present study, the effect of various anions, including Cl^-, NO_3^-, NO_2^-, and HCO_3^-, was investigated on the proposed process at 5 mM of matrix species under predetermined conditions (solution pH of 3, initial SY concentration of 50 mg/L, ZVI of 50 mg/L, H_2O_2 of 1 mM, PS of 1 mM, and reaction time of 30 min) (Fig. 6). As shown in Fig. 4, the decolorization effect is considerably inhibited by NO_2, while the scavenging effects by NO_3^-, Cl^-, and HCO_3^- were negligible on decolorization. This scavenging effect in the presence of different anions can be attributed to direct reaction of the scavengers with highly oxidant radicals (•OH and $SO_4^{\bullet -}$) and production form radicals with less oxidant power according to Eqs. (29–36) (Fan et al. 2015; Wu et al. 2019).

$Cl^- + SO_4^{\bullet -} \rightarrow SO_4^{2-} + Cl^{\bullet}$ (29)

$NO_3^- + SO_4^{\bullet -} \rightarrow SO_4^{2-} + NO_3^{\bullet}$ (30)

$NO_2^- + SO_4^{\bullet -} \rightarrow NO_2 + SO_4^{2-}$ (31)

$HCO_3^- + SO_4^{\bullet -} \rightarrow SO_4^{2-} + HCO_3^{\bullet}$ (32)

$Cl^- + \bullet OH \rightarrow HO^- + Cl^{\bullet}$ (33)

$NO_3^- + \bullet OH \rightarrow HO^- + NO_3^{\bullet}$ (34)

$NO_2^- + \bullet OH \rightarrow NO_2^{\bullet} + OH^-$ (35)

$HCO_3^- + \bullet OH \rightarrow H_2O + CO_3^{\bullet -}$ (36)

3.6 Scavenger tests

In this study, the radical scavenging experiments were conducted to differentiate the contributions of $SO_4^{\cdot -}$ and •OH for decolorization with methanol (EtOH) and tert-butyl alcohol (TBA). EtOH is a quencher of both •OH and $SO_4^{\cdot -}$ (k_{EtOH}, ·OH= (1.8–2.8) × $10^9 M^{-1}s^{-1}$, k_{EtOH}, $SO_4^{\cdot -}$ = (1.6–7.7) × $10^7 M^{-1}s^{-1}$). TBA is a strong quencher of •OH, and has 418–1900 times higher rate of reaction with than with $SO_4^{\cdot -}$ (k_{TBA}, ·OH= (3.8–7.6) ×$10^8 M^{-1}s^{-1}$, kTBA, $SO4^{\cdot -}$ = (4.0–9.1) × $10^5 M^{-1}s^{-1}$) (Qi et al. 2018). As shown in Fig. 7, without a quenching reagent, the complete decolorization was achieved within 30 min in the ZVI/PS/HP system. With the addition of 300 mM EeOH, the decolorization was decreased from 100–65% in 30 min. When TBA was introduced in the PS/ZVI/H_2O_2 system, the decolorization efficiency decreased from 100% to79% in 30 min, and hence the EtOH showed a stronger inhibitory effect than that of TBA. Therefore, both the $SO_4^{\cdot -}$ and •OH had important contributions to decolorization, while •OH was relatively more dominant than $SO_4^{\cdot -}$ for the decolorization in the PS-Z/nZVI system. The prominent contribution of hydroxyl radicals can be due to the reaction between SO_4 and water (Eq. (37)) or the reaction between ZVI and PS (Eq. (38)). Similar findings have been also reported by Yuan et al., 2014 (Yuan et al. 2014).

$SO_4^- + H_2O \rightarrow SO_4^{2-} + OH + H^+$ (37)

$S_2O_8^{2-} + Fe^0 + H_2O \rightarrow 2SO_4^{2-} + \bullet OH + Fe^{2+} + H^+$ (38)

3.7 Reusability and stability of ZVI particles

The stability and reusability of the catalyst as important factors can reduce the operational cost of such processes in large scale. For this reason, in the present study, the stability of the proposed catalyst was evaluated in five successive cycles under constant conditions (solution pH: 3, initial SY concentration: 50 mg/L, ZVI: 50 mg/L, H_2O_2: 1 mM, PS: 1 mM, and reaction time: 30 min). After every run, the catalyst was separated by an external magnet, washed three times with deionized water and dried at 80°C for 1 h, afterward, the dried catalyst was used for the next run of the experiments. (Fig. 8). As can be seen here, the catalytic activity of ZVI was constant in five consequent uses. The decolorization efficiency for the fifth run was as high as 80%. The decrease in ZVI efficiency can be attributed to the changes of the catalyst surface and deactivation of the catalyst by intermediates formed on the surface. Also, Fe^{2+} leaching can result in a decrease in active sites on the ZVI surface (Hussain et al. 2017; Kim et al. 2018). According to the results, it can be stated that the ZVI as a promising catalyst offers a high stability.

3.8 Mineralization

The aim of the degradation in the advanced oxidation technology is not only the pollutant degradation, but also the organic pollutant mineralization to CO_2 and H_2O completely (Yan et al. 2017). In addition, total organic carbon (TOC) directly reflected the change of organic matter content in aqueous solution. In this regard, the mineralization rate of the dye was determined through measuring the TOC concentration of the samples taken from the reactor at regular time intervals. Figure 10 presents dye degradation rate at solution pH 3, initial SY concentration 50 mg/L, ZVI 50 mg/L, H_2O_2 1 mM, and PS 1 mM. As can be seen in Fig. 9, the decolorization efficiency reached 100% after 30 min, while the mineralization of dye was 65% at that time. This difference in mineralization and removal rate can be attributed to the formation of intermediate compounds. Furthermore, comparing the degradation efficiency showed that a longer contact time is required to achieve the desired TOC degradation efficiency.

4 Conclusions

In this study, the Iron- zero valent particles(ZVI) was employed as a catalyst to activate persulfate (PS) and hydrogen peroxide (HP) for the removal of Sunset yellow (SY) from aqueous solutions using integrated H_2O_2/ZVI/PS process. According to the results, about 100% efficiency was obtained by the H_2O_2/ZVI/PS for dye removal at, pH: 3, ZVI: 50 mg/L, H_2O_2 dosage: 1 mM, PS dosage: 1 mM, and 30 min of reaction time. The kinetic study implied that the H_2O_2/ZVI/PS process followed the first-order kinetic model. The total organic carbon (TOC) test demonstrated that about 65% of mineralization was achieved after 30 min. The mechanistic study revealed that both $SO_4^{\bullet -}$ and •OH had a role in the decolorization during the H_2O_2/ZVI/PS system, while •OH showed a more dominant role compared to $SO_4^{\bullet -}$. Moreover, according to the results, ZVI particles offered a suitable performance after five cycles, which confirmed its high reusability. The decolorization efficiency by different processes including ZVI, PS, H_2O_2, ZVI/ H_2O_2, ZVI /PS, H_2O_2/ PS, and H_2O_2/ZVI/PS confirmed the strong synergistic effect among persulfate, H_2O_2, and catalyst, which play a substantial role in the decolorization. Therefore, the findings implied that H_2O_2/ZVI/PS system can be used as a valid method for the treatment of wastewaters contaminated with dye.

5 Declarations

Acknowledgement The authors would like to thank Farshid Ghanbari for his useful comment on the manuscript. This study was financially supported by Ahva JundishapurUniversity of Medical Sciences (Grant No. REC.1398.094).

Data Availability Data availability is not applicable.

Author's Contributions Mehdi Ahmadi contributed to the conception and design of the study. Rozhan Feizi conducted material preparation, data collection, and analysis. The first draft of the manuscript was

written by Rozhan Feizi, and all authors reviewed early drafts of the manuscript. All authors read and approved the final manuscript.

Funding

This work was supported by the Ahvaz Jundishapur University of Medical Sciences Grant No. REC.1398.094].

Compliance with Ethical Standards

Competing Interests The authors declare that they have no competing interests.

6 References

1. Anipsitakis GP, Dionysiou DD (2004) Radical generation by the interaction of transition metals with common oxidants. Environ Sci Technol 38:3705–3712. https://doi.org/10.1021/es035121o
2. Babuponnusami A, Muthukumar K (2012) Removal of phenol by heterogenous photo electro Fenton-like process using nano-zero valent iron. Sep Purif Technol 98:130–135. https://doi.org/10.1016/j.seppur.2012.04.034
3. Chang MC, Shu HY, Yu HH (2006) An integrated technique using zero-valent iron and UV/H2O2 sequential process for complete decolorization and mineralization of CI Acid Black 24 wastewater. J Hazard Mater 138:574–581. https://doi.org/10.1016/j.jhazmat.2006.05.088
4. Cui C, Jin L, Han Q, Lin K, Lu S, Zhang D, Cao G (2016) Removal of trace level amounts of twelve sulfonamides from drinking water by UV-activated peroxymonosulfate. Sci Total Environ 572:244–251. https://doi.org/10.1016/j.scitotenv.2016.07.183
5. de Souza Santos LV, Meireles AM, Lange LC (2015) Degradation of antibiotics norfloxacin by Fenton, UV and UV/H2O2. J Environ Manage 154:8–12. https://doi.org/10.1016/j.jenvman.2015.02.021
6. Desai NC, Chudasama JA, Karkar TJ, Patel BY, Jadeja KA, Godhani DR, Mehta JP (2016) Studies of styrene oxidation by catalyst based on zeolite-Y nanohybrid materials. J Mol Catal A Chem 424:203–219. https://doi.org/10.1016/j.molcata.2016.08.031
7. Fan Y, Ji Y, Kong D, Lu J, Zhou Q (2015) Kinetic and mechanistic investigations of the degradation of sulfamethazine in heat-activated persulfate oxidation process. J Hazard Mate 300:39–47
8. Feizi R, Ahmad M, Jorfi S, Ghanbari F (2019) Sunset yellow degradation by ultrasound/peroxymonosulfate/CuFe 2 O 4: Influential factors and degradation processes. Korean J Chem Eng 36:886–893. https://doi.org/10.1007/s11814-019-0268-0
9. Guo P, Tang L, Tang J, Zeng G, Huang B, Dong H, Zhang Y, Zhou Y, Deng Y, Ma L (2016) Catalytic reduction–adsorption for removal of p-nitrophenol and its conversion p-aminophenol from water by gold nanoparticles supported on oxidized mesoporous carbon. J Colloid Interface Sci 469:78–85. https://doi.org/10.1016/j.jcis.2016.01.063

10. Hou L, Zhang H, Xue X (2012) Ultrasound enhanced heterogeneous activation of peroxydisulfate by magnetite catalyst for the degradation of tetracycline in water. Sep Purif Technol
11. : 147 – 52. https://doi.org/10.1016/j.seppur.2011.06.023
12. Hussain I, Li M, Zhang Y, Li Y, Huang S, Du X, Liu G, Hayat W, Anwar N (2017) Insights into the mechanism of persulfate activation with nZVI/BC nanocomposite for the degradation of nonylphenol. Chem Eng J 311:163–172. https://doi.org/10.1016/j.cej.2016.11.085
13. Ike IA, Linden KG, Orbell JD, Duke M (2018) Critical review of the science and sustainability of persulphate advanced oxidation processes. Chem Eng J 338:651–669. https://doi.org/10.1016/j.cej.2018.01.034
14. Khan JA, He X, Khan HM, Shah NS, Dionysiou DD (2013) Oxidative degradation of atrazine in aqueous solution by UV/H2O2/Fe2+, UV/S2O82-/Fe2 + and UV/HSO5-/Fe2 + processes: a comparative study. Chem Eng J 218:376–383. https://doi.org/10.1016/j.cej.2012.12.055
15. Kim C, Ahn JY, Kim TY, Shin WS, Hwang I (2018) Activation of persulfate by nanosized zero-valent iron (NZVI): mechanisms and transformation products of NZVI. Environ Sci Technol 52:3625–3633. https://doi.org/10.1021/acs.est.7b05847
16. Li J, Ji Q, Lai B, Yuan D (2017) Degradation of p-nitrophenol by Fe0/H2O2/persulfate system: Optimization, performance and mechanisms. J Taiwan Inst Chem Eng 80:686–694. https://doi.org/10.1016/j.jtice.2017.09.002
17. Li Y, Hsieh WP, Mahmudov R, Wei X, Huang C (2013) Combined ultrasound and Fenton (US-Fenton) process for the treatment of ammunition wastewater. J Hazard Mater 244:403–411. https://doi.org/10.1016/j.jhazmat.2012.11.022
18. Maroudas A, Pandis PK, Chatzopoulou A, Davellas LR, Sourkouni G, Argirusis C (2020) Synergetic decolorization of azo dyes using ultrasounds, photocatalysis and photo-fenton reaction. Ultrason Sonochem 71:105367. https://doi.org/10.1016/j.ultsonch.2020.105367
19. Matyszczak G, Krzyczkowska K, Fidler A (2020) A novel, two-electron catalysts for the electro-Fenton process. J Water Process Eng 36:101242. https://doi.org/10.1016/j.jwpe.2020.101242
20. Matzek LW, Carter KE (2016) Activated persulfate for organic chemical degradation: a review. Chemosphere 151:178–188. https://doi.org/10.1016/j.chemosphere.2016.02.055
21. Oh SY, Kang SG, Chiu PC (2010) Degradation of 2, 4-dinitrotoluene by persulfate activated with zero-valent iron. Sci Total Environ 408:3464–3468. https://doi.org/10.1016/j.scitotenv.2010.04.032
22. Oh SY, Kang SG, Kim DW, Chiu PC (2011) Degradation of 2, 4-dinitrotoluene by persulfate activated with iron sulfides. Chem Eng J 172:641–646. https://doi.org/10.1016/j.cej.2011.06.023
23. Oh SY, Kim HW, Park JM, Park HS, Yoon C (2009) Oxidation of polyvinyl alcohol by persulfate activated with heat, Fe2+, and zero-valent iron. J Hazard Mater 168:346–351. https://doi.org/10.1016/j.jhazmat.2009.02.065
24. Qi C, Yu G, Huang J, Wang B, Wang Y, Deng S (2018) azole degradation. Chem Eng J 353:490–498. https://doi.org/10.1016/j.cej.2018.07.056

25. Raji M, Mirbagheri SA, Ye F, Dutta J (2020) Nano zero-valent iron on activated carbon cloth support as Fenton-like catalyst for efficient color and COD removal from melanoidin wastewater. Chemosphere 263:127945. https://doi.org/10.1016/j.chemosphere.2020.127945
26. Malakootiana M, Asadzadehc SN (2020) Oxidative removal of tetracycline by sono Fenton-like oxidation process in aqueous media. Desalination Water Treat 193:392–401. doi 10.5004/dwt.2020.25810
27. Tang J, Tang L, Feng H, Zeng G, Dong H, Zhang C, Huang B, Deng Y, Wang J, Zhou Y (2016) pH-dependent degradation of p-nitrophenol by sulfidated nanoscale zerovalent iron under aerobic or anoxic conditions. J Hazard Mater 320:581–590. https://doi.org/10.1016/j.jhazmat.2016.07.042
28. Tariq M, Khan J (2020) Inquest of efficient photo-assist advanced oxidation processes (AOPs) for removal of azo dye (acid yellow 17) in aqueous medium: a comprehensive study on oxidative decomposition of AY 17. SN Appl Sci 2:1–12. https://doi.org/10.1007/s42452-020-03701-2
29. Wang JL, Xu LJ (2012) Advanced oxidation processes for wastewater treatment: formation of hydroxyl radical and application. Crit Rev Environ Sci Technol 42:251–325. https://doi.org/10.1080/10643389.2010.507698
30. Wordofa DN, Walker SL, Liu H (2017) Sulfate radical-induced disinfection of pathogenic Escherichia coli O157: H7 via iron-activated persulfate. Environ Sci Technol Lett 4:154–160. https://doi.org/10.1021/acs.estlett.7b00035
31. Wu J, Wang B, Blaney L, Peng G, Chen P, Cui Y, Deng S, Wang Y, Huang J, Yu G (2019) Degradation of sulfamethazine by persulfate activated with organo-montmorillonite supported nano-zero valent iron. Chem Eng J 361:99–108. https://doi.org/10.1016/j.cej.2018.12.024
32. Yan J, Qian L, Gao W, Chen Y, Ouyang D, Chen M (2017) Enhanced Fenton-like degradation of trichloroethylene by hydrogen peroxide activated with nanoscale zero valent iron loaded on biochar. Sci Rep 7:1–9. https://doi.org/10.1038/srep43051
33. Yuan S, Liao P, Alshawabkeh AN (2014) Electrolytic manipulation of persulfate reactivity by iron electrodes for trichloroethylene degradation in groundwater. Environ SciTechnol 48:656–663. https://doi.org/10.1021/es404535q
34. Zha S, Cheng Y, Gao Y, Chen Z, Megharaj M, Naidu R (2014) Nanoscale zero-valent iron as a catalyst for heterogeneous Fenton oxidation of amoxicillin. Chem Eng J 255:141–148. https://doi.org/10.1016/j.cej.2014.06.057
35. Zhao S, Ma H, Wang M, Cao C, Xiong J, Xu Y, Yao S (2010) Study on the mechanism of photo-degradation of p-nitrophenol exposed to 254 nm UV light. J Hazard Mater 180:86–90. https://doi.org/10.1016/j.jhazmat.2010.03.076

Figures

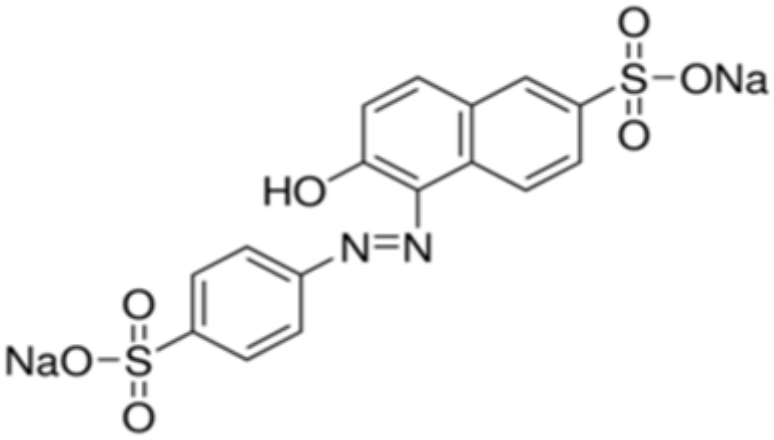

Figure 1

The structural formula of Sunset Yellow

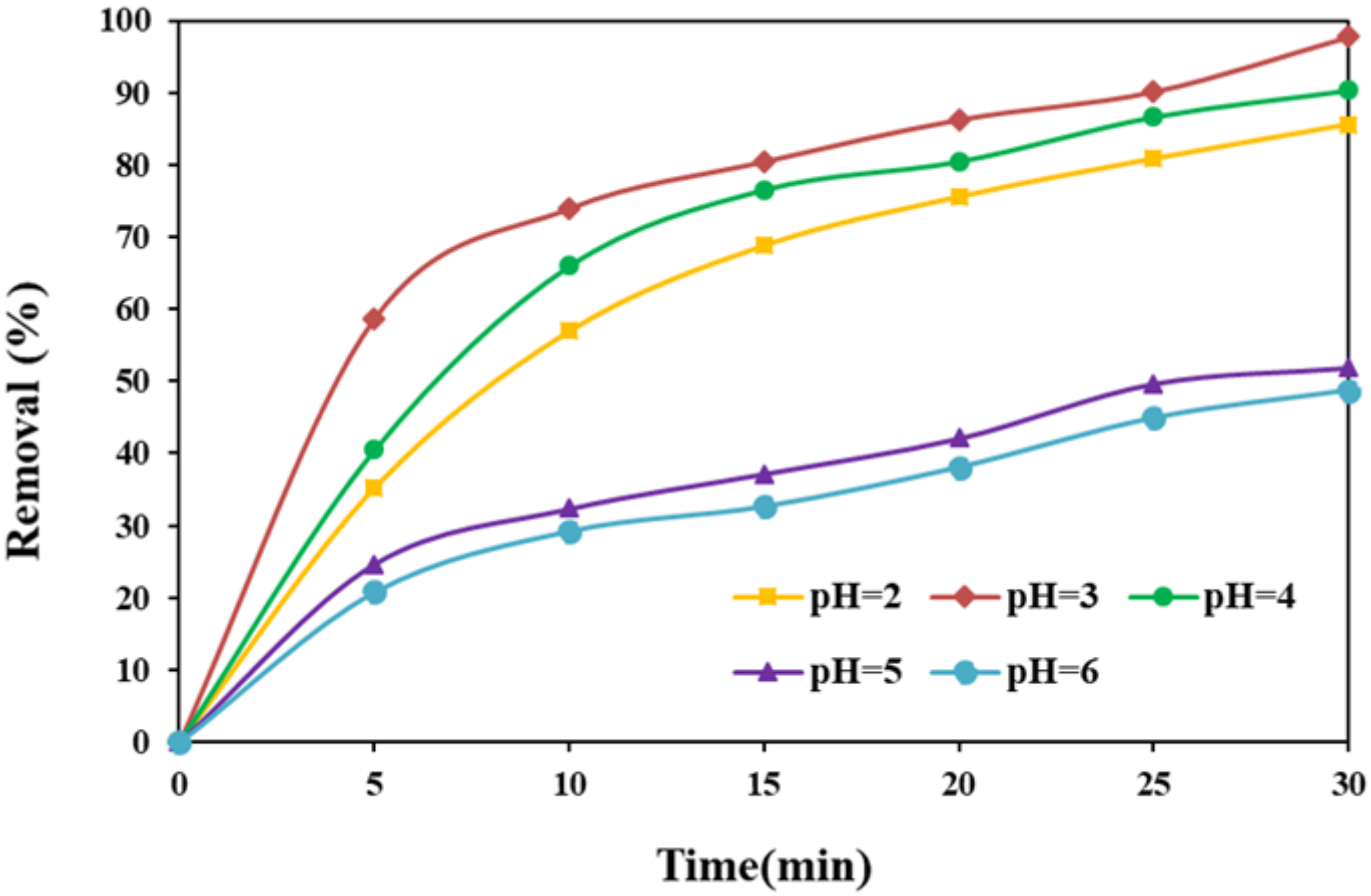

Figure 2

Effect of solution pH on SY removal (initial SY concentration: 50 mg/L, ZVI 50: mg/L, H2O2 concentration: 1 mM, and PS concentration:1 mM)

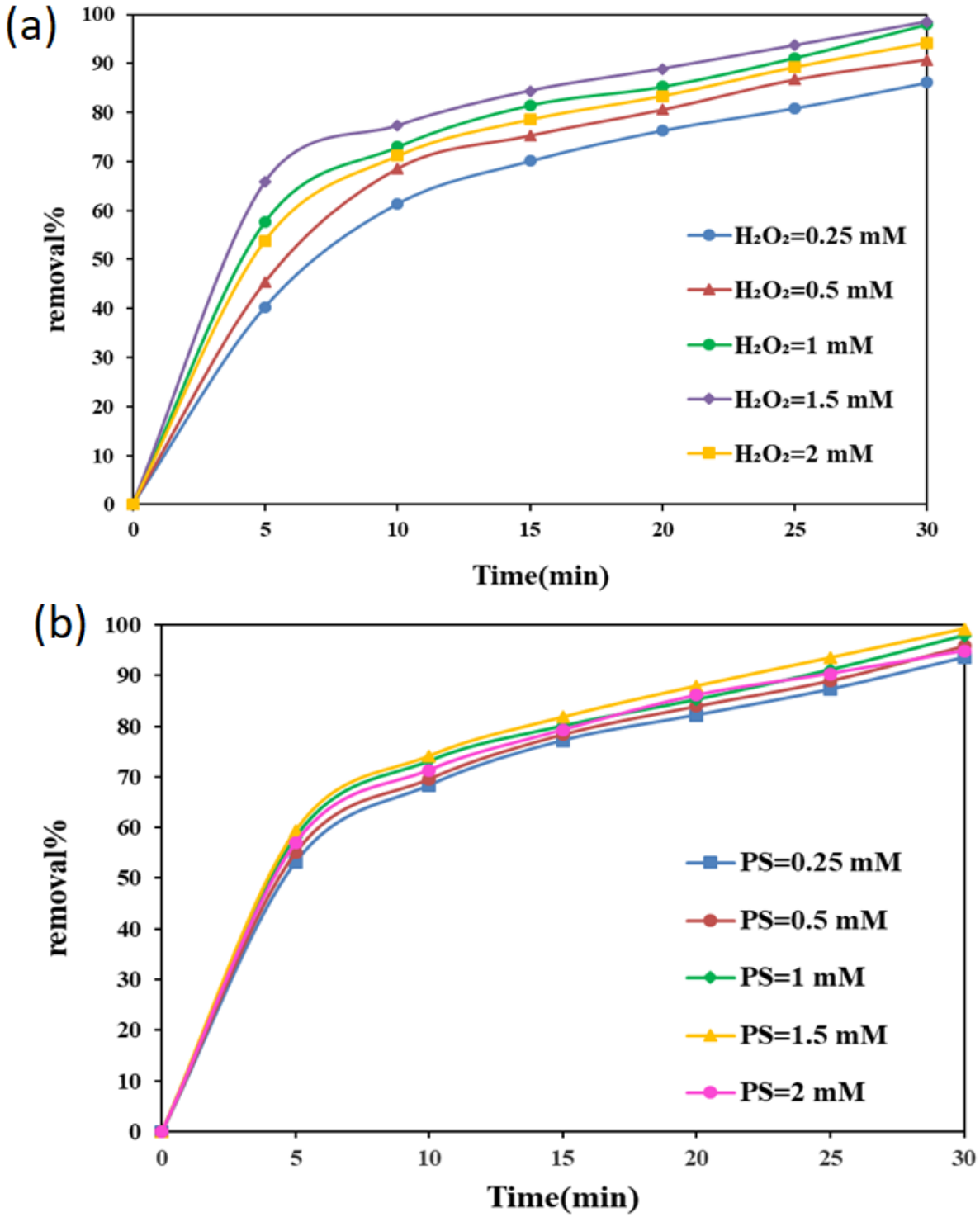

Figure 3

a Effect of H2O2 concentration on SY removal (initial SY concentration of 50 mg/L solution pH= 3, ZVI 50 mg/L, and PS concentration of 1 mM), and b. Effect of PS concentration on SY removal (initial SY concentration of 50 mg/L solution pH= 3, ZVI 50 mg/L, and H2O2 concentration of 1 mM)

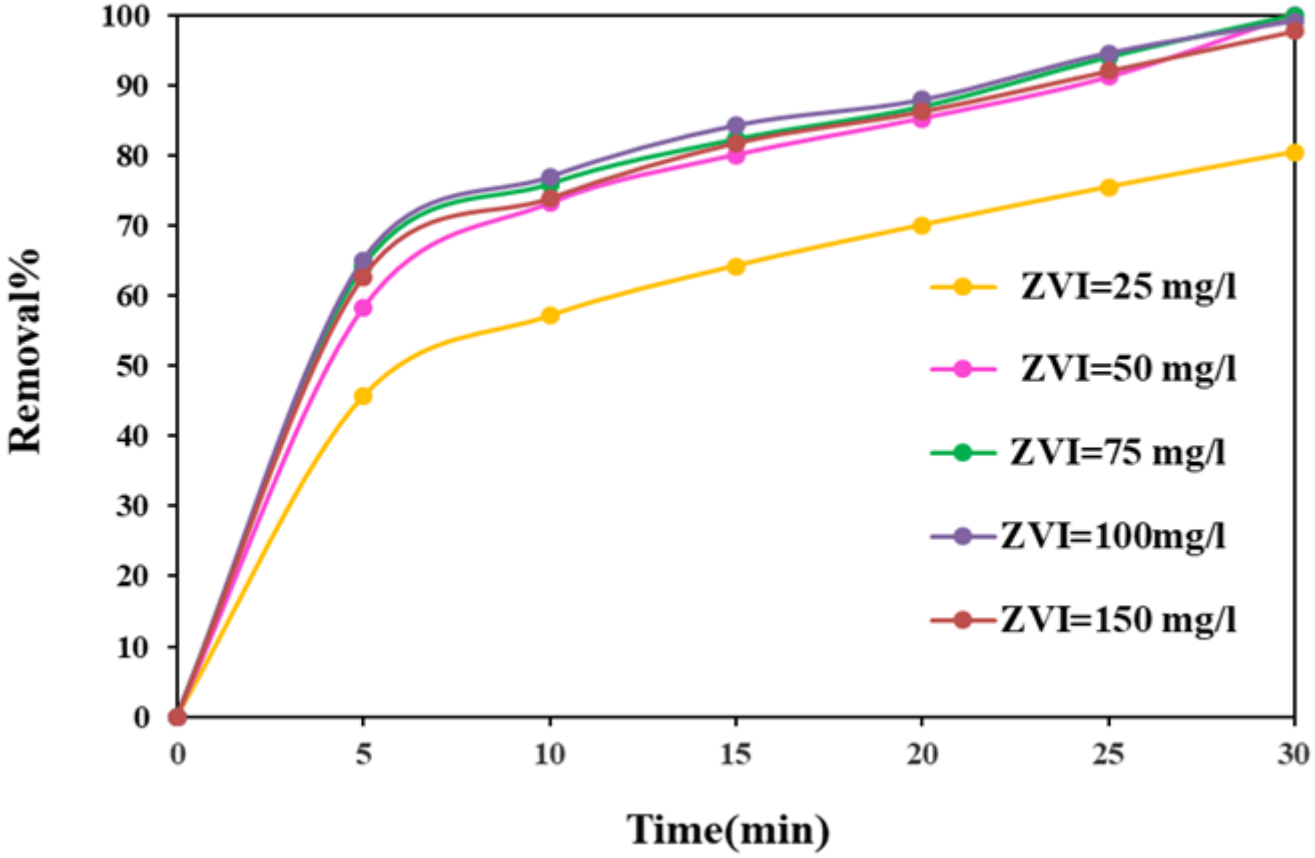

Figure 4

Effect of ZVI dose on SY removal (initial SY concentration of 50 mg/L solution pH 3, H2O2 concentration of 1 mM, and PS concentration of 1 mM)

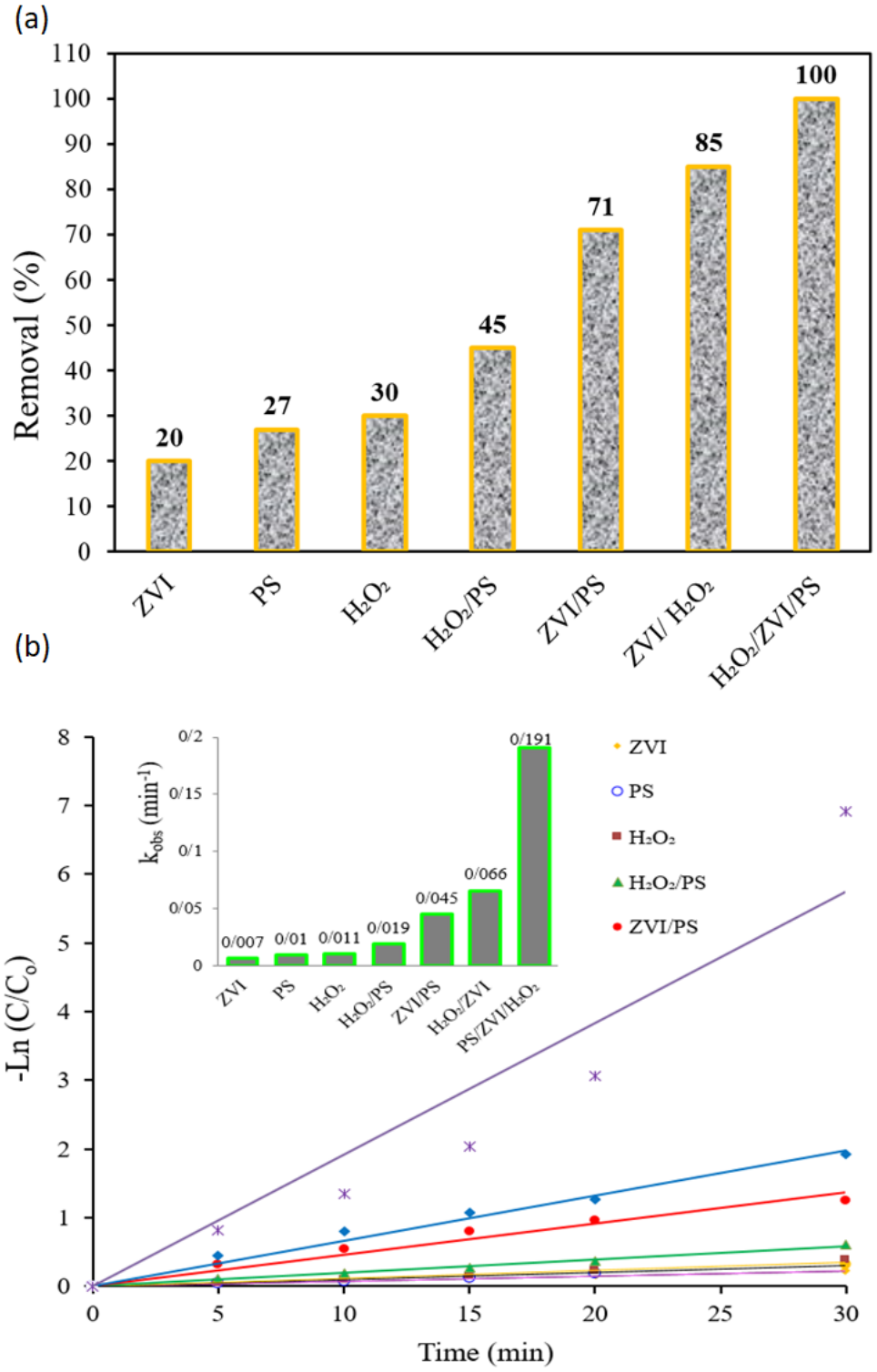

Figure 5

(a) Role of other alternatives in SY removal and (b) The linear form of first order kinetic (solution pH 3, initial SY concentration 50 mg/L, ZVI 50 mg/L, H2O2 1 mM, PS 1 mM, and reaction time 30 min).

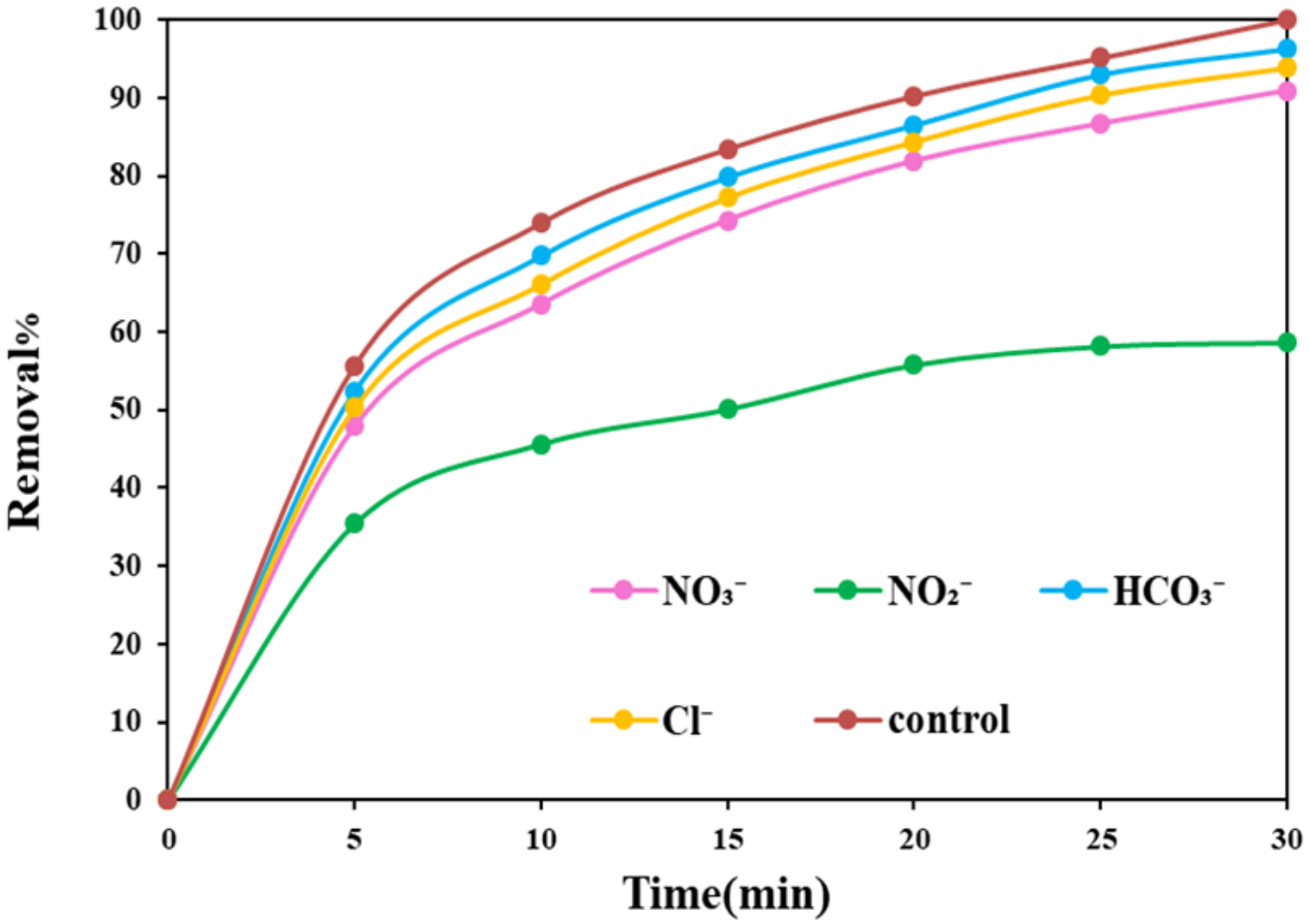

Figure 6

The effect of different anions on the ZVI/H2O2/PS process (solution pH 3, initial SY concentration 50 mg/L, ZVI 50 mg/L, H2O2 1 mM, and PS 1 mM).

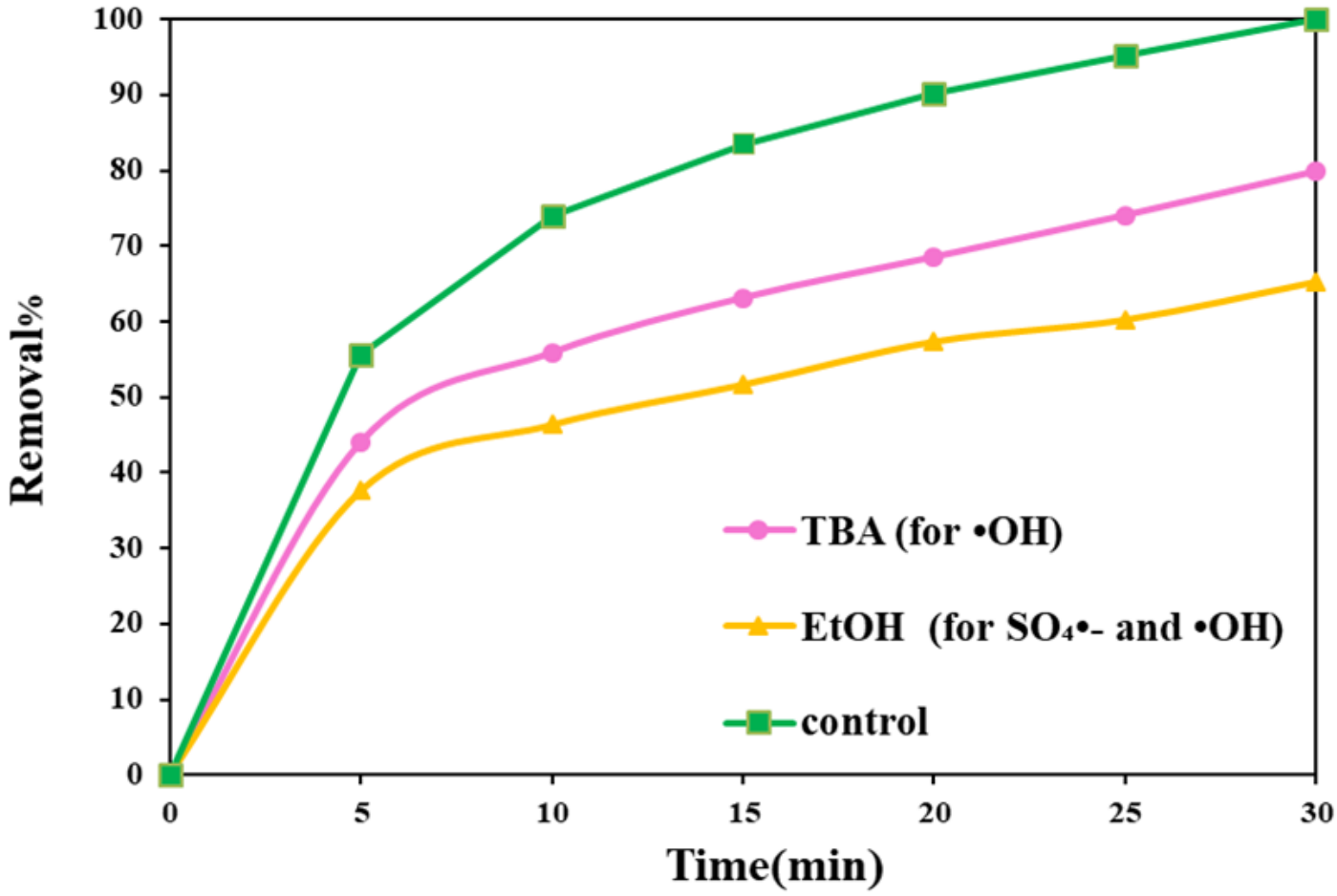

Figure 7

The effect of scavengers (TBA and EtOH) on the H2O2/ZVI/PS process (solution pH 3, initial SY concentration 50 mg/L, ZVI 50 mg/L, H2O2 1 mM, and PS 1 mM,).

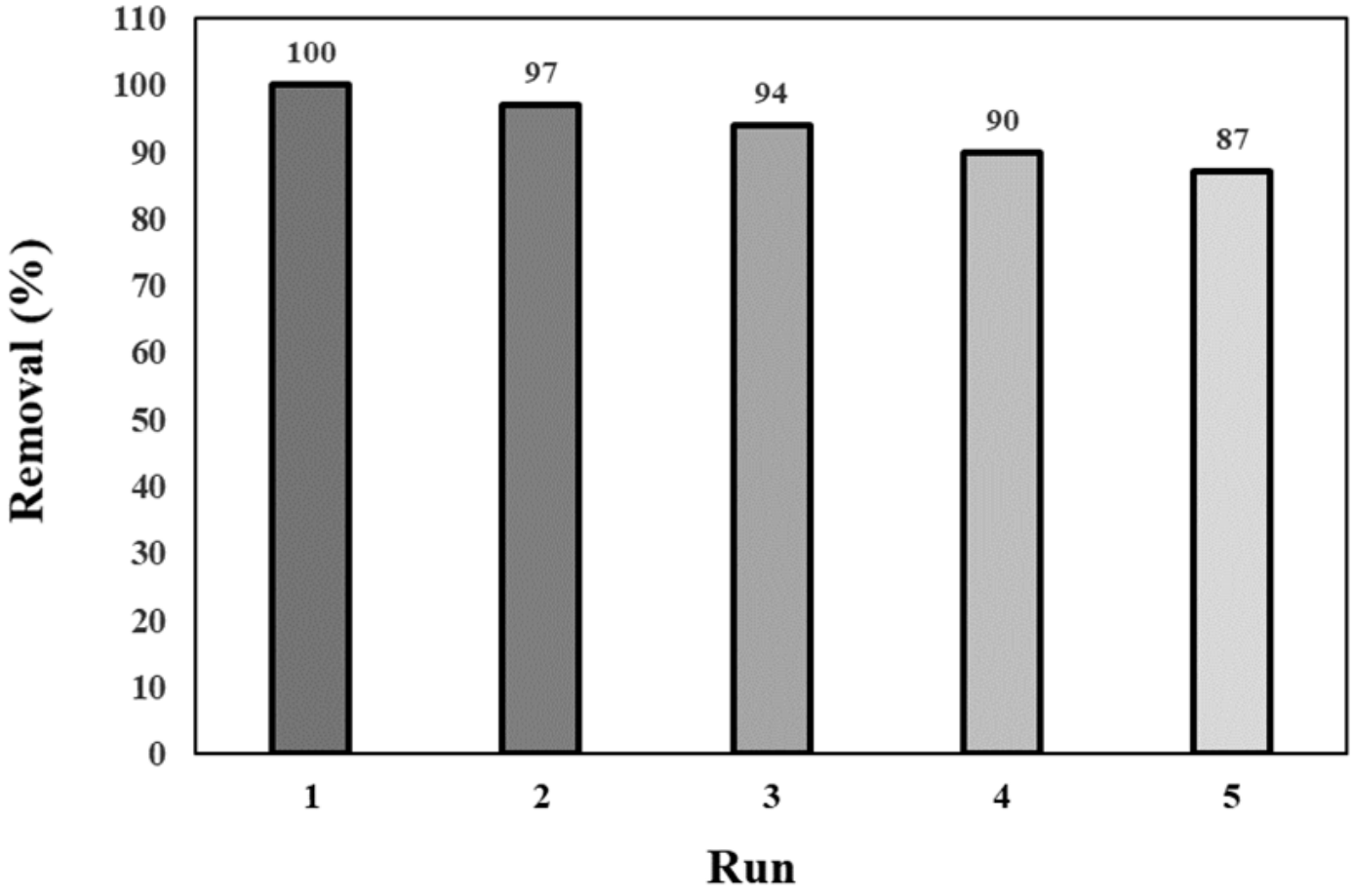

Figure 8

Reusability of ZVI after five consecutive cycles at solution pH 3, initial SY concentration 50 mg/L, ZVI 50 mg/L, H2O2 1 mM, and PS 1 mM,).

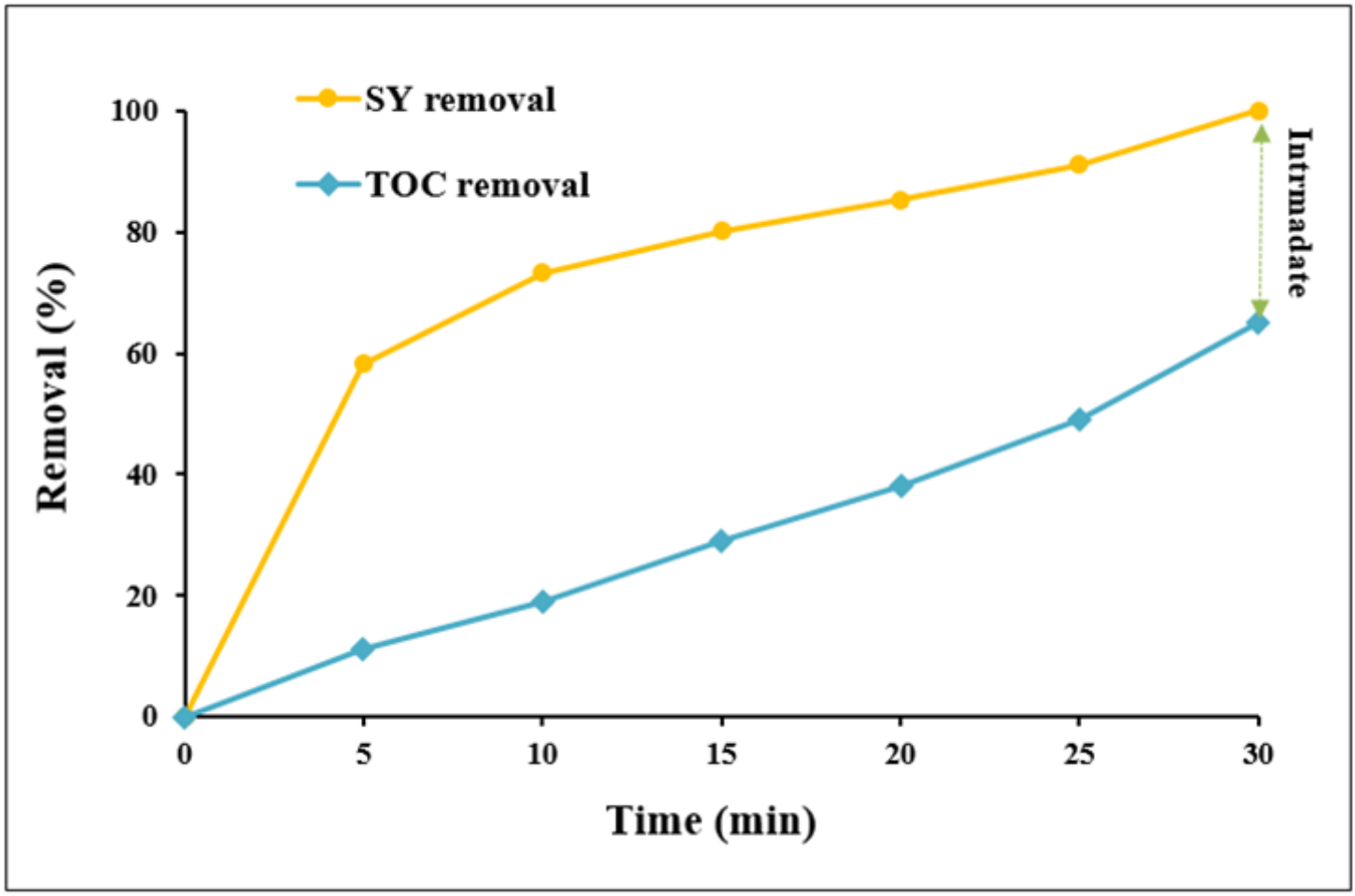

Figure 9

TOC removal of SY in the H2O2/ZVI/PS process (solution pH 3, initial SY concentration 50 mg/L, nZVI 50 mg/L, H2O2 1 mM, and PS 1 mM,).

Supplementary Files

This is a list of supplementary files associated with this preprint. Click to download.

- Graphicalabstract.png